COORDINATION COMPLEX [Eu(μ_2-OC_2H_5)(btfa)(NO_3) (phen)]$_2$·phen WITH HIGH LUMINESCENT EFFICIENCY

Mihail S. Iovu[1], Victor I. Verlan*[1], Ion P. Culeac[1], Olga Bordian[1], Vera E. Zubareva[2], Ion Bulhac[2], Marius Enachescu[3], Nichita A. Siminel[1], and Anatol V. Siminel[1]

[1]Institute of Applied Physics, Academiei str.5, Chisinau, MD-2028 Republic of Moldova
[2]Institute of Chemistry, Academiei str.3, Chisinau, MD-2028 Republic of Moldova
[3]University Politehnica Bucharest, Splaiul Independentei 313, Bucharest, 060042 Romania
E-mail: vverlan@gmail.com

(Received February 18, 2021)

https://doi.org/10.53081/mjps.2021.20-1.06 *CZU:535.33:543.4*

Abstract

Experimental results on the bis[(μ_2-etoxi)(benzoyl trifluoroacetonato)(nitrato)(1,10-phenantroline)europium(III)]1,10-phenantroline europium(III) coordination complex (hereafter, [Eu(μ_2-OC_2H_5)(btfa)(NO_3)(phen)]$_2$·phen) are described. The complex is characterized by photoluminescence (PL) and infrared spectroscopy. Photoluminescence spectra of the complex exhibit strong emission with specific narrow emission bands associated with the $^5D_0 \rightarrow {}^7F_j$ (j = 0–4) transitions. The pattern of emission band splitting and the luminescence time decay suggest the presence of at least two different sites of the Eu^{3+} ion in a low-symmetry environment. The absolute PL quantum yield of the complex is determined to be 49.2%.

Keywords: rare-earth compounds, europium (III) complex, luminescence, quantum yield.

Rezumat

Sunt prezentate rezultate experimentale pentru complexul coordinativ al europiului III) - [Eu(μ_2-OC_2H_5)(btfa)(NO_3)(phen)]$_2$phen. Complexul a fost caracterizat prin spectroscopia de fotoluminescență și spectroscopia în infraroșu. Spectrele de fotoluminescență ale complexului reprezintă benzi de emisie puternice asociate cu tranzițiile $^5D_0 \rightarrow {}^7F_j$ (j=0-4). Caracterul despicării benzilor de emisie, cât și timpul de relaxare al luminescenței indică prezența a cel puțin două site-uri diferite ale ionului Eu^{3+} în mediu cu simetrie redusă. A fost determinat randamentul cuantic absolut al complexului de 49,2%.

Cuvinte cheie: compuși de pământ rar, complex Europium (III), luminescență, randament cuantic.

1. Introduction

Rare-earth compounds, and specifically their coordination complexes, attract a lot of interest because of their fundamental physical properties and numerous applications in different

fields in optoelectronics, biotechnology, biochemistry, medicine, and other industries [1–3]. Complexes with trivalent europium ion Eu^{3+}exhibit high fluorescence efficiency upon UV excitation, emission spectra in the visible range with high color purity and a large Stokes shift, long-lived luminescence, etc. [4–6]. This luminescence is characterized by long lifetimes and sharp spectral lines. In biomedical field, europium(III) complexes are extensively used for the development of high-performance sensors, luminescent labels in immunoassays, bioanalysis, etc. [7]. Europium ions are characterized by a simple structure of $^{2S+1}L_J$ multiplets with non-degenerate first excited and ground levels, $^5D_0$ and $^7F_0$. Because of these specific properties of trivalent europium ion, it can be used as a luminescent probe to acquire information on the local symmetry in crystalline host matrices or glasses as well as complexes with organic ligands [8–10].

In the recent years, increased research efforts have been focused on new lanthanide complexes with potential development toward material sciences, chemical and biomedical applications, quantum storage devices, etc. [11, 12]. Previously, we reported preliminary results on Eu(III) coordination compound bis[(μ_2-etoxi)(benzoyl trifluoroacetonato)(nitrato)(1,10-phenantroline)europium(III)]1,10-phentroline, hereafter [Eu(μ_2-OC_2H_5)(btfa)(NO_3)(phen)]$_2$·phen [13]. This work reports a further study of photoluminescence (PL) properties of europium(III) coordination complex [Eu(μ_2-OC_2H_5)(btfa)(NO_3)(phen)]$_2$·phen.

2. Preparation and Characterization of the Complex

Europium(III) coordination complex [Eu(μ_2-OC_2H_5)(btfa)$(NO)_3$(phen)]$_2$·phen has been synthesized as described elsewhere [14]. Samples were characterized by infrared (IR) and PL spectroscopy. Infrared spectra were registered using a PerkinElmer Spectrum 100 FTIR Spectrometer at a resolution of 1 cm^{-1}. Infrared spectra were recorded on a dry powder between KBr pellets (4000–650 cm^{-1}) or in Nujol mull (4000–400 cm^{-1}) between KBr pellets. Photoluminescence emission spectra were recorded using a single emission monochromator MDR-23 and different excitation sources (337 or 405 nm) close to ligand absorption maximum. Photoluminescence spectral measurements were carried out using a Thorlabs LD Model CPS405 4.5 mW as an excitation source. A 337-nm pulsed nitrogen laser at a repetition rate of 10–100 Hz and a pulse width of 10 ns was used for PL relaxation measurements. Photoluminescence signal was detected in a photon counting mode using a Hamamatsu H8259-01 module with a C8855-01 counting unit connected to a PC. The spectral resolution for PL measurements was as low as 0.125 nm. For both the PL spectra and the quantum yield measurements, the emission spectra were corrected for the instrument spectral sensitivity. The luminescence time decay was recorded using a nitrogen pulsed laser as a light source at a repetition rate of 10 Hz. The H8259-01 PMT module with a C8855-01 pulse-counter provides time-resolved measurements at a resolution of 50 μs, which is sufficient for registration of PL relaxation in a range of 50 μs to 10 ms.

The [Eu(μ_2-OC_2H_5)(btfa)$(NO)_3$(phen)]$_2$·phen complex exhibits a bright-red emission under UV irradiation. Figure 1 shows a photographic image of a powder sample under day-light illumination compared with the sample under UV irradiation. Measurements of absolute PL quantum yield were performed using the absolute method of integration sphere [15]. The integration sphere was 150 mm in diameter. The inner spherical cavity wall was coated with MgO (extremely high diffuse reflectance) using a burning magnesium ribbon in an O_2 stream. The sphere was mounted in front of an MDR-23 monochromator. Absolute quantum yield Q is

defined as the ratio of the number of emitted photons N_{em} to the number of absorbed photons [16]:

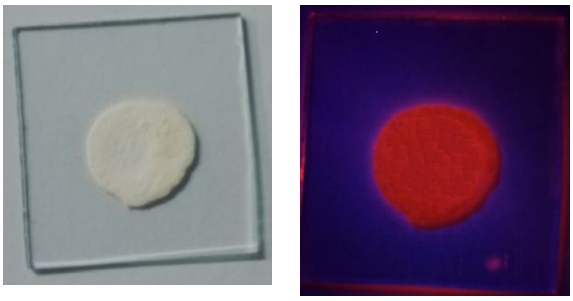

Fig. 1. Photographic image of a powder sample: (left) under day-light illumination and (right) under UV irradiation.

$$Q = N_{em} / N_{abs} .$$

Figure 2 illustrates the experimental approach for measuring the absolute quantum yield. First, the excitation spectrum is registered when the substrate is placed under a direct excitation beam in a sample holder. The total area under this spectrum (S_0) is proportional to the number of excitation photons minus those absorbed in the substrate. In the next step, the excitation spectrum is registered when the substrate with a PL compound is placed under an excitation beam in a sample holder. The area under this spectrum (S_1) is proportional to the number of excitation photons minus those absorbed in the substrate and the compound. The PL emission spectrum was registered with a probe (substrate with the sample powder) placed inside a sample holder. The area under the PL spectrum (S_2) is proportional to the number of emission photons under direct and diffuse excitation. Finally, the PL spectrum is registered when the probe is excited only by indirect excitation light diffusively reflected from the integrating sphere walls (S_3). The quantum yield is determined as $Q = (S_2 - S_3)/(S_0 - S_1)$ [15, 16].

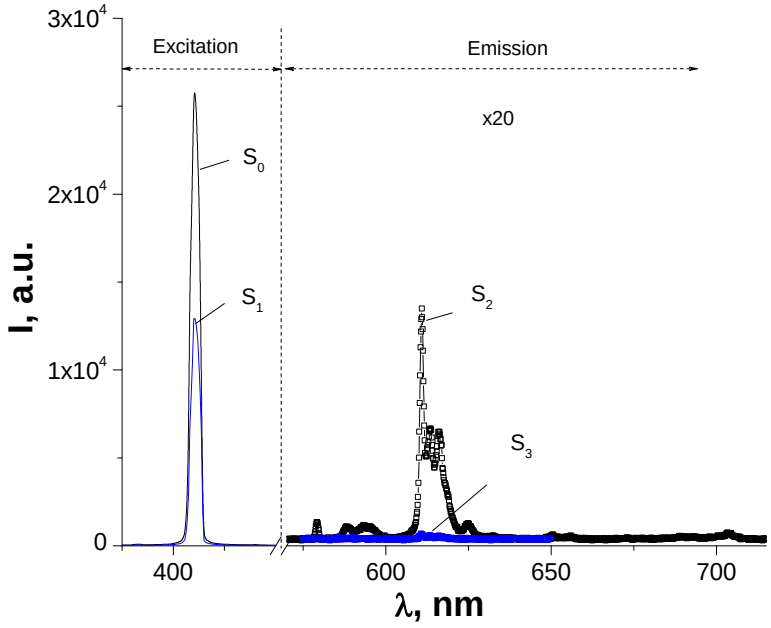

Fig. 2. Illustration of the spectra for the determination of quantum yield: S_0 is the excitation spectrum registered with the substrate under an excitation beam in a sample holder; S_1 is the excitation spectrum registered with a probe under an excitation beam; S_2 is the PL emission spectrum registered with the probe under an excitation beam; and S_3 is the PL emission spectrum registered when the probe is excited by indirect excitation light diffused by the integration sphere walls.

3. Infrared Transmission Spectra

Infrared spectra were registered using a PerkinElmer Spectrum 100 FTIR Spectrometer with at a resolution of 1 cm^{-1}. Infrared spectra were recorded on a dry powder between KBr pellets (4000–650 cm^{-1}) or in Nujol mull between KBr pellets (4000–400 cm^{-1}). Absorption bands in the IR spectrum were identified by comparing with the reference data [17, 18]. The absorption bands corresponding to the basic structural units of the $[Eu(\mu_2\text{-}OC_2H_5)(btfa)(NO)_3(phen)]_2 \cdot phen$ complex are listed in Table 1.

Table 1. Ligands absorption bands in the complex related to the basic structural units

Ligand	**Structural unit**	**ν, cm^{-1}**
btfa	ν(C=O)	1610
	$\nu_{as}(CF_3)$	1180
	$\nu_s(CF_3)$	1135
	δ(CH)	731; 700
o-phen	ν(C=N)	1637
	ν(C=C)	1675; 1498; 1441
OC_2H_5	$\nu_{as}(CH_2/CH_3)$	1459
	$\nu_{as}CH_2/CH_3)$	1377
	Scissor oscillation CH_2	1470
	$\delta(CH_2)$	1466
NO_3	NO^-_3	1489; 1290; 1026

4. Photoluminescence Emission Spectra

Photoluminescence emission spectra were registered for both the powdered samples and the samples dissolved in a dimethylformamide solution under excitation of a 405-nm or 337-nm laser beam. The PL emission spectrum registered at 300 K in the powder sample (λ_{exc} 405 nm) is shown in Fig. 3a. Upon UV excitation, the Eu^{3+} complex exhibits well-known characteristic transitions $^5D_0 \rightarrow {}^7F_j$ (j = 0, 1, 2, 3, 4) with typical narrow band components. The complex shows strong emission bands in the solid state; less intense bands are registered in the dimethylformamide solution (Fig. 3b).

Less resolved Stark splitting and wider peaks of the emission bands are known to be a common feature of Eu(III) complexes in solution [21]. This difference in the degree of splitting suggests different degrees of distortion of the ligand crystal field in different media. With a decrease in temperature, the peak intensity of the basic emission bands increases and the resolution of emission band splitting also increases. Assignment of the emission lines is consistent with the predicted number of transition bands, which is based on the selection rules for low-symmetry complexes [19]. The strongest emission is related to the transition between excited state $^5D_0$ and ground state manifold $^7F_2$ due to an efficient energy transfer from higher excited states to $^5D_0$ [20]. Along with the transitions from the first excited state $^5D_0$, a number of extremely weak transitions from the higher excited state level $^5D_1$ can be observed (Fig. 3a): $^5D_1$–$^7F_0$ (526.8 nm), $^5D_1$–$^7F_1$ (533–543 nm), $^5D_1$–$^7F_2$ (551–573 nm), and $^5D_1$–$^7F_3$ (583 nm).

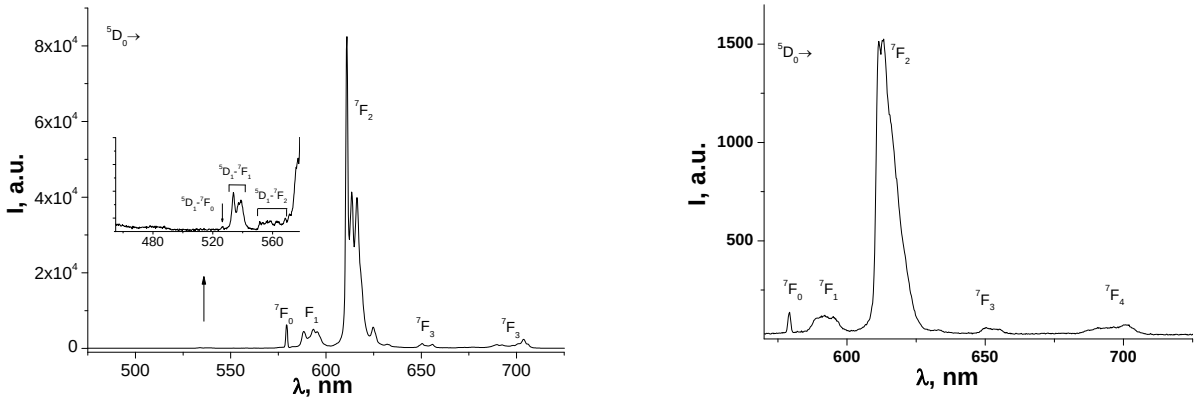

Fig. 3. Illustration of the PL spectrum of the europium(III) complex under 405-nm excitation (T = 300 K): (a) PL spectrum for the powder sample; the integrated intensity ratio is R = 9.02 and (b) PL spectrum of the complex in a dimethylformamide solution; the integrated intensity ratio is R = 14.4.

The band at ~580 nm represents the forbidden electric dipole transition $^5D_0\rightarrow{}^7F_0$, from the $^5D_0$ excited state to the $^7F_0$ ground state. The $^5D_0\rightarrow{}^7F_0$ transition is forbidden by the selection rules and commonly can be observed only in low-symmetry complexes, if the lanthanide ion is located on a site with C_{nv}, C_n, or C_s symmetry [8, 19]. It is one of the most remarkable features in the luminescence spectrum of the $[Eu(\mu_2\text{-}OC_2H_5)(btfa)(NO)_3(phen)]_2\cdot phen$ complex. Since both the emitting $^5D_0$ and ground state $^7F_0$ of the transition are non-degenerate and cannot be split by the ligand field, the number of its components exactly indicates the number of different Eu^{3+} ion sites [19]. The band at 580 nm has a small line width, which at 300 K equals 32 cm^{-1} for the powder sample and 45 cm^{-1} for the solution sample (Figs. 3, 4). Although the low-resolution spectrum for the $^5D_0\rightarrow{}^7F_0$ transition reveals an almost symmetrical single line (Fig. 5), its

relatively wide full width at half maximum suggests that it can contain two closely spaced components. In fact, deconvolution of the emission band $^5D_0 \rightarrow {}^7F_0$ (Fig. 5) reveals two lines, and this is consistent with the assumption of existence of two different sites of the Eu^{3+} ion.

The $^5D_0 \rightarrow {}^7F_1$ transition with the emission band at 587–600 nm is a purely magnetic dipole transition; it represents the crystal field splitting of the $^7F_1$ level. An important feature of this transition is that its integrated intensity is relatively insensitive to the local crystal field induced by ligands surrounding the Eu^{3+} ion. Therefore, the $^5D_0 \rightarrow {}^7F_1$ transition is used as a reference in comparing the absolute emission intensities within the Eu(III) spectrum [8, 10]. The pattern of splitting of the $^5D_0 \rightarrow {}^7F_1$ transition provides information to which crystal system the complex corresponds. In the case of complexes with low symmetry (orthorhombic or lower symmetries) the maximum splitting of three lines appears [8, 19]. In Fig. 6, we can distinguish the $^5D_0 \rightarrow {}^7F_1$ splitting into more than six components (peaks and shoulders), which can be attributed to the existence of at least two distinct, although chemically quite similar, emitting Eu^{3+} centers in the complex [22, 23].

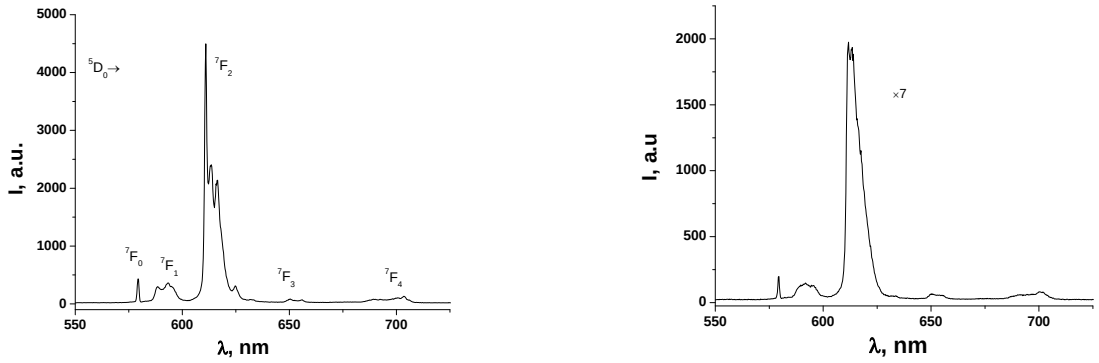

a *b*

Fig. 4. Photoluminescence spectrum of the europium(III) complex under 337-nm excitation (T = 300 K): (a) PL spectrum for the powder sample; the integrated intensity ratio is R = 7.18 and (b) PL spectrum of the complex in a dimethylformamide solution; the integrated intensity ratio is R = 11.

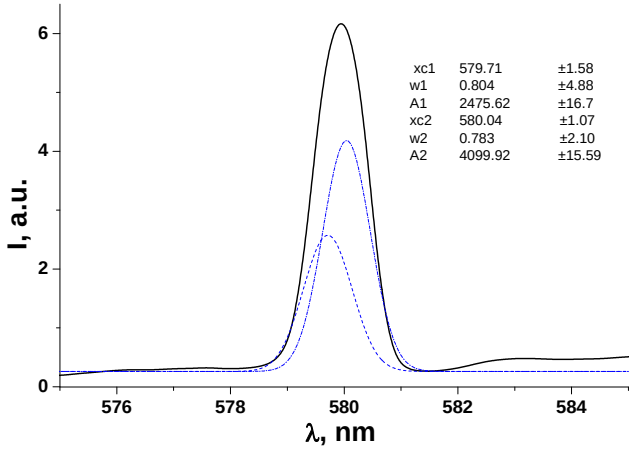

Fig. 5. Deconvolution of the emission band at ~580 nm attributed to the $^5D_0 \rightarrow {}^7F_0$ transition in the case of the powder sample (T = 300 K, λ_{exc} = 405 nm).

The dominant feature in the PL spectrum of the $[Eu(\mu_2\text{-}OC_2H_5)(btfa)(NO)_3(phen)]_2\cdot phen$ compound is the $^5D_0 \rightarrow {}^7F_2$ electric dipole transition with the emission band at 610–630 nm (Fig. 6). It is this transition that is responsible for the typical bright red luminescence observed in most of the europium(III) compounds. Since its intensity is sensitive to the local symmetry of the Eu^{3+} ion and the nature of the ligands, the $^5D_0 \rightarrow {}^7F_2$ transition is considered as a "hypersensitive" transition [8–10]. The PL spectrum of the $[Eu(\mu_2\text{-}OC_2H_5)(btfa)(NO)_3(phen)]_2\cdot phen$ compound shows that the $^5D_0 \rightarrow {}^7F_2$ transition is much more intense than the $^5D_0 \rightarrow {}^7F_1$ magnetic dipole transition (Figs. 4, 6). The asymmetric ratio *R*, which is defined as an integrated intensity ratio $I_2(^5D_0 \rightarrow {}^7F_2)/I_1(^5D_0 \rightarrow {}^7F_1)$ is equal to 9.02 for the powdered sample; for the sample dissolved in a dimethylformamide solution, the ratio is 14.4 (λ_{exc} = 405 nm). This high magnitude of asymmetric ratio *R* suggests that the Eu(III) ion is not at an inversion center [19]. At a low temperature of 10.7 K, the $^5D_0 \rightarrow {}^7F_2$ transition splitting into at least ten components and shoulders can be observed; this multiple splitting is consistent with the existence of at least two sites of the Eu(III) ion.

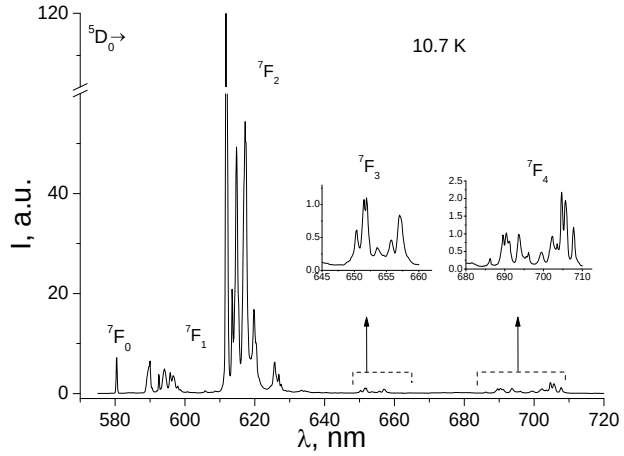

Fig. 6. Photoluminescence spectrum for the powder $[Eu(\mu_2\text{-}OC_2H_5)(btfa)(NO)_3(phen)]_2\cdot phen$ sample measured at 10.7 K. The insets show the splitting of the $^7F_3$ and $^7F_4$ bands. The excitation light is 405 nm.

The other two emission bands corresponding to the $^7F_3$, and $^7F_4$ levels, which are electric dipole transitions, are extremely weak. The $^5D_0 \rightarrow {}^7F_3$ transition at 640–655 nm is a forbidden electric dipole transition, which is the weakest in the spectrum of the compound. This transition can only gain intensity via J-mixing [10]. Another electric dipole transition is the $^5D_0 \rightarrow {}^7F_4$ emission band at 680–710 nm. The $^5D_0 \rightarrow {}^7F_4$ transition is slightly higher than the $^5D_0 \rightarrow {}^7F_3$ transition. It is considered to be sensitive to the Eu^{3+} environment, because the intensity of the $^5D_0 \rightarrow {}^7F_4$ transition is determined not only by symmetry factors, but also by the chemical composition of the host matrix [23–25].

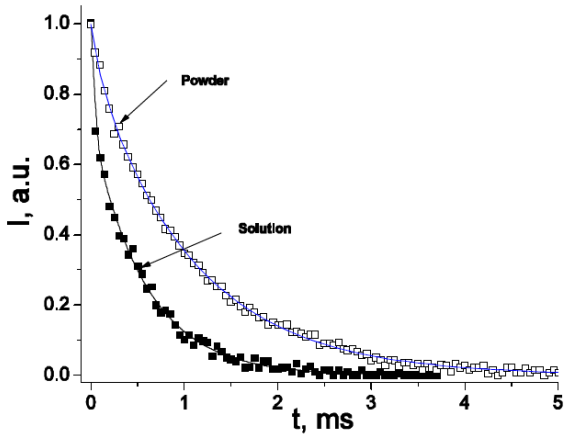

Fig. 7. Photoluminescence decay profiles for the powder and dissolved sample of the $[Eu(\mu_2\text{-}OC_2H_5)(btfa)(NO_3)(phen)]_2 \cdot phen$ complex at 300 K registered at 611 nm under 337-nm pulsed excitation [13].

Photoluminescence decay curves of the complex were registered at 300 K for the $^5D_0 \rightarrow {}^7F_2$ transition at 611 nm. Temporal characteristics of the PL exhibit a bi-exponential decay for both the powder sample and the sample dissolved in a dimethylformamide solution (Fig. 8). The PL decay curves can be fitted by the two-exponential function:

$$I(t) = A_1 \exp(-t/\tau_1) + A_2 \exp(-t/\tau_2),$$

where A_1 and A_2 are pre-exponential factors; τ_1 and τ_2 are the time constants.

The lifetime constants for Eu^{3+} obtained from the plot in Fig. 8 are τ_1 = 0.67 ms and τ_2 = 0.82 ms for the powdered sample and τ_1 = 0.28 ms and τ_2 = 0.57 ms for the complex dissolved in a dimethylformamide solution [13]. The absolute quantum yield of PL measured in the powder samples by the integration sphere was determined to be 49.2%, while the sensitization efficiency was 89.3%.

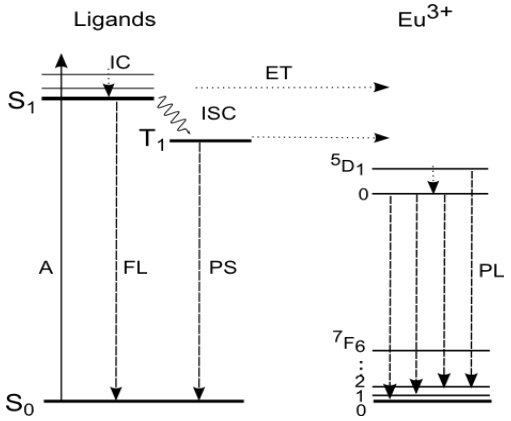

Fig. 8. Illustration of the mechanism of energy transfer from the organic ligand to the Eu^{3+} ion: S_0, S_1, and T_1 are the singlet ground state, singlet excited state, and triplet state, respectively. A is absorption, FL is fluorescence, PS is phosphorescence, IC is internal conversion, ISC is intersystem crossing, and ET is energy transfer.

Photoluminescence spectra can be interpreted in terms of energy transfer from organic ligands to the Eu(III) ion [10, 23]. Figure 8 illustrates the mechanism of energy transfer from organic ligands to the Eu(III) ion. Under UV radiation, the organic ligand of the complex is excited from the singlet ground state S_0 to a vibration level of the first excited singlet state S_1. There are three possible deactivation transitions of excited electrons from the singlet S_1 state. These transitions are as follows: (i) radiative transitions from excited singlet state S_1 to ground state S_0, which contribute to the ligand molecule fluorescence and the excitation of 4*f* shell electrons through the Foerster mechanism; (ii) non-radiative transitions from singlet state S_1 to triplet state T_1; and (iii) a Dexter transition of excited electrons from the S_1 level to the 4*f* shell levels of the Eu^{3+} ion. Triplet state T_1 can be deactivated similarly to the S_1 state, which results in the phosphorescence of the ligand molecule (Foerster mechanism), or through intramolecular energy transfer from the T_1 state to the 4*f* level of the Eu^{3+} ion (Dexter mechanism), which results in Eu^{3+} luminescence emission [19–22].

Further studies will be performed to extend the described preliminary PL results. Currently, research is progressing on powder pattern X-ray diffraction measurements aimed at the structural characterization of the compound.

5. Conclusions

The $[Eu(\mu_2\text{-}OC_2H_5)(btfa)(NO)_3(phen)]_2{\cdot}phen$ complex has been characterized by IR and PL spectroscopy. Upon UV excitation, the Eu^{3+} complex exhibits well-known characteristic transitions $^5D_0 \rightarrow {}^7F_j$ (j = 0–4) with typical narrow emission bands. Although the $^5D_0 \rightarrow {}^7F_0$ transition represents a single line, its full width at half maximum is relatively large of about 32 cm^{-1}; this fact suggests that it can contain two closely spaced components. Both the emission spectra and the PL decay characteristics indicate the presence of two different sites of the Eu^{3+} ion. The absolute PL quantum yield and the sensitization efficiency have been determined to be 49.2 and 89.3%, respectively. We believe that this high luminescence material can be useful for various applications in optoelectronics.

Acknowledgments. This work was supported by the ANCD National Research Program (project no. 20.80009.5007.14, project no. 20.80009.5007.28).

References

[1] Lanthanide Luminescence: Photophysical, Analytical and Biological Aspects, Springer Series on Fluorescence, Methods and Applications, Ed. by Pekka Hanninen and Harri Harma, Springer-Verlag, Berlin, Heidelberg, vol. 7, 2011. DOI: 10.1007/4243-2010-3

[2] J.-C. G. Bunzli, A.-S. Chauvin, C. D. B. Vandevyver, Song Bo, and S. Comby, Ann. N. Y. Acad. Sci. 1130, 97 (2008). DOI: 10.1196/annals.1430.010 9

[3] S. V. Eliseeva, and J.-C. G. Bunzli, Chem. Soc. Rev. 39, 189 (2010).

[4] Lanthanide Probes in Life, Chemical and Earth Sciences: Theory and Practice, Ed. by J.-C.G. Bunzil and G.R. Choppin, Elsevier, Amsterdam–Oxford–New York–Tokyo, 1989.

[5] A. P. Demchenko, Introduction to Fluorescence Sensing, Second Edition, Springer International Publishing, Switzerland, 2015. ISBN 978-3-319-20779-7 ISBN 978-3-319-20780-3 (eBook), DOI: 10.1007/978-3-319-20780-3

[6] Fluorescence Spectroscopy in Biology. Advanced Methods and their Applications to Membranes, Proteins, DNA, and Cells, Springer Series on Fluorescence, vol. 3: Methods and Applications, Ed. by M. Hof, R. Hutterer, and V. Fidler, Springer-Verlag, Berlin, Heidelberg, 2005.
[7] P. R. Selvin, Annu. Rev. Biophys. Biomol. Struct. 31, 275 (2002), DOI: 10.1146/annurev.biophys.31.101101.140927
[8] K. Binnemans, Coord. Chem. Rev. 295, 1 (2015).
[9] J.-C. G. Bünzli and G. O. Pradervand, J. Chem. Phys. 85, 2489 (1986), DOI: 10.1063/1.451057
[10] G. Blasse and B.C. Grabmaier, Luminescent Materials, Springer-Verlag, Berlin, Heidelberg, 1994.
[11] (a) Guangfu Li, Dongxia Zhu, Xinlong Wang, Zhongmin Su, and Martin R. Bryce, Chem. Soc. Rev. 49, 765 (2020); (b) J. J. Baldoví and A. Kondinski, Inorganics 6 (4), 101 (2018); DOI:10.3390/inorganics6040101; (c) D. Aguilà, L. A Barrios, V. Velasco, O. Roubeau, A. Repollés, P. J. Alonso, J. Sesé, S. J. Teat, F. Luis, and G. Aromí, J. Am. Chem. Soc. 136 (40), 14215 (2014), DOI: 10.1021/ja507809w; (d) Monatsh. Chem. Chem. Mon. 145 (12), 1913 (2014).
[12] L. Armelao, D. Belli Dell'Amico, L. Bellucci, G. Bottaro, S. Ciattini, L. Labella, G. Manfroni, F. Marchetti, C.A. Mattei, and S. Samaritani, Eur. J. Inorg. Chem. 2018 (40), 4421 (2018). DOI:10.1002/ejic.201800747
[13] V. I. Verlan, I. P. Culeac, O. Bordian, V. E. Zubareva, I. F. Bulhac, M. S. Iovu, M. Enachescu, N. A. Siminel, and V.V. Nedelea, Luminescence Properties of a Novel Eu^{3+} Dinuclear Coordination Compound. In: I. Tiginyanu, V. Sontea, and S. Railean (Eds.), 4th Int. Conf. on Nanotechnologies and Biomedical Engineering, ICNBME 2019, IFMBE Proc., vol. 77, Springer, Cham. DOI:10.1007/978-3-030-31866-6-33
[14] (a) O. Bordian, V. Verlan, I. Culeac, M. Iovu, I. Bulhac, and V. Zubarev, Synthesis, Absorption and Photoluminescence Properties of the New Coordination Compound $Eu(DBM)_3(Ph_3PO)_1H_2O$, Advanced Topics in Optoelectronics, Microelectronics, and Nanotechnologies IX, Ed. by M. Vladescu, R. Tamas, and I. Cristea, Proc. of SPIE, vol. 10977, 109771E, 2018 SPIE CCC code: 0277-786X/18/$18, DOI: 10.1117/12.2323761;
(b) O. Bordian, V. Verlan, I. Culeac, M. Iovu, I. Bulhac, V. Zubarev, and M. Enachescu, Certificat de prioritate OSIM, Romania, A/0000 din 07-01-2019, Compus coordonativ al Eu(III) de tip dinuclear cu liganzi micsti avind proprietati de luminiscenta si procedeu de obtinere.
[15] K. Rurack, Fluorescence Quantum Yields: Methods of Determination and Standards, Springer Series on Fluorescence, 2008, vol. 5, pp. 101–145, Springer-Verlag, Berlin, Heidelberg, Published online: March 11, 2008, DOI:10.1007/4243 2008 019
[16] A.K. Gaigalas and L. Wang, J. Res. Natl. Inst. Stand. Technol. 113, 17 (2008).
[17] L. J. Bellamy, The Infrared Spectra of Complex Molecules, Methuen & Co. LTD, Willey, London, New York, 1971.
[18] K. Nakamoto, Infrared and Raman Spectra of Inorganic and Coordination Compounds, Wiley, New York, 1978, p. 239.
[19] J.-C.G. Bunzli, Lanthanide probes. In: Lanthanide Probes in Life, Chemical and Earth Sciences: Theory and Practice, Ed. by J.-C.G. Bunzil and G. R. Choppin, Elsevier, Amsterdam–Oxford–New York–Tokyo, 1989, Ch. 7.
[20] J. Georges and J. M. Mermet, Spectrochim. Acta, Part A, 49 (3), 397 (1993).
[21] L. N. Puntus, I. S. Pekareva, K. A. Lyssenko, A. S. Shaplov, E. I. Lozinskaya, A. T. Zdvizhkov, M. I. Buzin, and Y. S. Vygodskii, Opt. Mater. 32, 707 (2010).

[22] M. H. V. Werts, Luminescent Lanthanide Complexes: Visible Light Sensitised Red and Near-Infrared Luminescence, University of Amsterdam, Thesis (2000), Library of the University of Amsterdam, Digital Academic Repository, Amsterdam, The Netherlands.
[23] K. Binnemans, R. Van Deun, C. Gorller-Walrand, S. R. Collinson, F. Martin, D. W. Bruceand, and C. Wickleder, Phys. Chem. Chem. Phys. 2, 3753 (2000), DOI: 10.1039/b003379k
[24] J.-C. G. Bunzli and S. V. Eliseeva, Basics of Lanthanide Photophysics, In: Lanthanide Luminescence: Photophysical, Analytical, and Biological Aspects, Ed. by P. Hanninen and H. Harma, Springer Series on Fluorescence (2010), Springer-Verlag, Berlin, Heidelberg, 2010, DOI:10.1007/4243-2010-3
[25] Ye Jin, Jiahua Zhang, Shaozhe Lu, Haifeng Zhao, Xia Zhang, and Xiao-jun Wang, J. Phys. Chem. C 112, 5860 (2008).
26. I. P. Culeac, V. I. Verlan, O. Bordian, V. E. Zubareva, I. F. Bulhac, M. S. Iovu, M. Enachescu, N. A. Siminel, and A.V. Siminel, Synthesis and characterization of novel photoluminescent Eu(III) dinuclear coordination compound, submitted for publication in J. Phys. Chem.